Absence of isotopic dependence in the sub-barrier fusion of ^{48}Ti+ ^{58,60,64}Ni systems

A. M. Vinodkumar and K. M. Varier
Department of Physics, Calicut University, Calicut - 673 635, India

N. V. S. V. Prasad and D. L. Sastry
Department of Nuclear Physics, Andhra University, Visakhapatnam - 530 003, India

A. K. Sinha, N. Madhavan, P. Sugathan, D. O. Kataria, and J. J. Das
Nuclear Science Centre, P B No. 10502, New Delhi -110 067, India

(Received 18 May 1995)

Fusion process in the near and sub-barrier region has been investigated for the systems ^{48}Ti+ ^{58,60,64}Ni using the heavy-ion reaction analyzer (HIRA). Fusion excitation functions and the mean angular momenta are obtained from the measured evaporation residue cross sections. Significant enhancements both in the cross section and mean angular momentum data are seen with respect to the predictions of the one-dimensional barrier penetration model. Simplified coupled channel calculations incorporating linear coupling to the inelastic channels (lowest 2^+ and 3^- states of both the projectile and the target) are not able to explain the observed enhancements. A systematic analysis of the data indicates lack of isotopic dependence in the sub-barrier fusion for these three systems.

PACS number(s): 25.70.Jj, 24.10.Eq

I. INTRODUCTION

The heavy-ion fusion in the energy region around the Coulomb barrier continues to be a topic of interest. The basic motivation revolves around the question of understanding the mechanism underlying the observed enhancement of sub-barrier fusion cross sections compared to the predictions of the one-dimensional barrier penetration model (1D BPM) [1–4]. Investigations of the role of multidimensional evolution of the fusion process in the barrier region indicate a rich

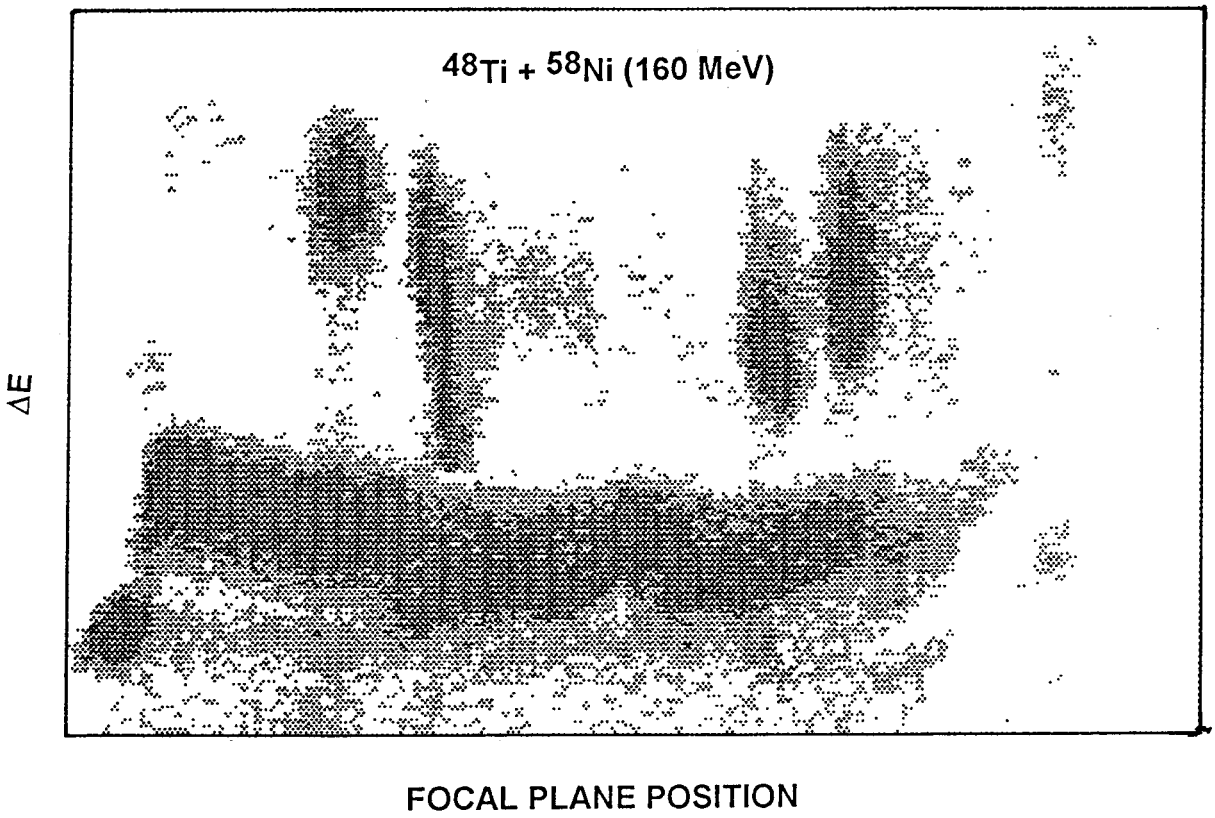

FIG. 1. Two-dimensional plot of MWPC ΔE vs focal plane position for particles detected at the focal plane of the HIRA, for the reaction ^{48}Ti+ ^{58}Ni at 160 MeV. The evaporation residues are in the upper half of the plot, while the scattered beamlike particles are in the lower half.

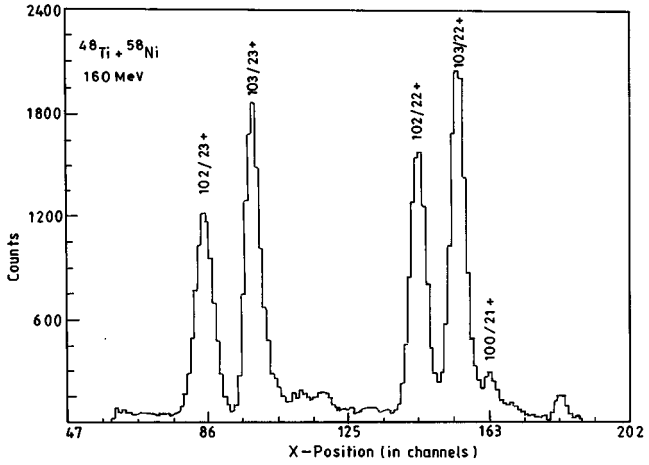

FIG. 2. M/q spectrum (position spectrum) generated by putting a gate on the evaporation residues in Fig. 1.

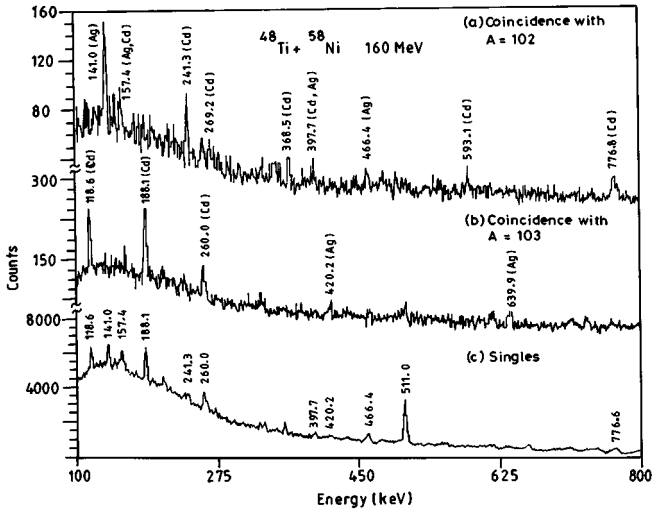

FIG. 3. γ-ray spectra from the evaporation residues in the reaction ^{48}Ti+^{58}Ni at 160 MeV. (a) Gated by mass 102; (b) gated by mass 103; (c) singles spectrum. The well-identified γ lines of relevant isotopes are indicated.

interplay of the nuclear structure and the reaction dynamics resulting in a revival of detailed experimental and theoretical studies of various aspects of the heavy-ion reaction mechanism near the Coulomb barrier. Several recipes and models have been proposed incorporating the multidimensional effects, though a comprehensive theory has yet to emerge. The theoretical approaches attempted so far consider the use of energy and spin-dependent potential to account for the energy-dependent path of evolution in the fusion process [5], inclusion of effects of the zero-point motion [6], the static deformation [7], the neck formation [8], and the coupling of important reaction channels to the entrance channel [9,10].

There have been several studies of the isotopic dependence of the fusion observables (mainly the cross sections) in the barrier region. Strong isotopic dependence is seen in a few cases, whereas in other cases the dependence turns out to be rather mild. In the case of $^{144-154}$Sm isotopes [7], the increase in the static deformation with mass number A is seen to relate well with the observed cross-section enhancement. Excitation functions (in some cases also the spin distributions) have been measured for systems involving isotopes of Zr, Ni, Cu, Mo, Ru, Rh, and Sn with various projectiles [1–4]. Nickel isotopes (58, 60, and 64) have been investigated thoroughly using a large number of projectiles [11–15]. The observed behavior may be classified into two groups. The first group, consisting of projectiles ^{28}Si, ^{32}S, ^{35}Cl, and ^{58}Ni, shows isotopic dependence, while the second group, consisting of projectiles ^{30}Si, ^{36}S, ^{37}Cl, and ^{64}Ni, shows very little dependence, if any. The origin of these effects [16] has been investigated using the coupled channel approach. A possible role of transfer couplings has been identified, although a quantitative explanation has not been possible in most of the cases because of the nonavailability of the data on transfer cross sections in the barrier region. Further, an exhaustive test of the underlying channel coupling effects demands a measurement of other fusion observables such as moments of the spin distribution. A limited test of the theoretical ideas has been possible so far because mostly fusion excitation functions alone are available.

A program to measure fusion and transfer for the ^{48}Ti+^{58,60,64}Ni systems has been undertaken with the objective of studying the isotopic dependence of the fusion cross sections for the Ni isotopes in the barrier region. We report, in this paper, the measurements of the cross sections and mean spins in the barrier region for the fusion of ^{48}Ti with ^{58,60,64}Ni and comparison with other studies involving Ni isotopes as targets. Simplified coupled channel calculations have been performed and compared with the experimental data.

II. EXPERIMENTAL DETAILS AND DATA ANALYSIS

Experiments were carried out using ^{48}Ti beams ($E_{\rm lab}$=126–168 MeV) provided by the 15UD Pelletron ac-

TABLE I. Comparison of detection efficiencies (in percentages) as obtained by the γ coincidence method with those obtained by a convolution of particle-parameter distributions with the HIRA transmission. Errors are typically 10% of the values indicated for PACE2 results. Errors for the experimental data are given in parentheses.

	3N			4N		
	^{58}Ni	^{60}Ni	^{64}Ni	^{58}Ni	^{60}Ni	^{64}Ni
γ coincidence method	7.7 (1.7)	7.1 (1.5)	9.3 (2.6)	4.6 (2.1)	6.1 (0.6)	11.7 (1.0)
PACE2	6.8	8.0	11.3	6.0	10.9	13.1

TABLE II. Fusion cross sections for the ^{48}Ti+Ni systems.

^{48}Ti+^{58}Ni		^{48}Ti+^{60}Ni		^{48}Ti+^{64}Ni	
$E_{\text{c.m.}}$ (MeV)	σ_{fus} (mb)	$E_{\text{c.m.}}$ (MeV)	σ_{fus} (mb)	$E_{\text{c.m.}}$ (MeV)	σ_{fus} (mb)
72.73	0.14(0.01)	72.87	0.25(0.03)	71.59	0.14(0.01)
73.83	0.55(0.04)	73.99	1.18(0.10)	72.74	0.74(0.65)
74.90	1.41(0.1)	75.01	3.54(0.30)	73.89	2.68(0.20)
76.01	4.87(0.3)	76.11	9.67(0.55)	75.01	14.5(0.75)
76.97	11.9(0.7)	77.16	27.2(1.5)	75.96	30.6(1.5)
77.93	22.5(1.0)	78.14	48.5(2.5)	77.00	48(2.5)
78.94	37.2(2.0)	79.19	78(4)	78.17	62(3)
80.00	57.2(2.95)	80.29	109(6)	79.32	118(6)
81.05	86.0(4.2)	81.38	166(9)	80.40	143(9)
82.06	123(5.5)	82.42	204(10)	81.56	193(9.5)
84.23	188(9)	83.53	232(10.5)	82.69	245(12.5)
86.38	263(12)	85.75	308(15)	83.81	293(17)
88.54	369(19.5)	87.97	373(16)	84.95	322(15.5)
90.74	384(19)	90.19	416(21.5)	86.09	361(17)
		92.43	446(23)	88.37	406(21)
				90.68	401(22.5)
				92.98	473(26)
				95.28	495(27.5)

celerator at the Nuclear Science Centre (NSC), New Delhi. Isotopically enriched targets of ^{58}Ni (99.8%), ^{60}Ni(99.83%) and ^{64}Ni (98%) of thicknesses 330, 273, and 242 μg cm^{-2}, respectively, were used. The measurements were carried out using the heavy-ion reaction analyzer (HIRA) [17]. Two silicon surface barrier detectors, at $\pm 30°$ were used for beam flux normalization. A high purity germanium (HPGe) detector of 23% relative efficiency and resolution of $\sim$2 keV at 1.332 MeV, was placed at 90° to the beam direction for detection of γ rays. The focal plane detector system [18] consisted of a 200 mm$\times$60 mm position-sensitive multiwire proportional counter (MWPC) followed by a 180 mm deep split-anode ionization chamber with an active area of 120 mm$\times$35 mm.

Several measurements were done at 160 MeV to obtain the calibration of position at the focal plane, the HIRA detection efficiency, charge state and recoil energy distributions, and the angular distribution of the evaporation residues (ER's). The position calibration and the determination of the dependence of detection efficiency on focal plane position was done by varying the HIRA fields to sweep a particular mass peak across the focal plane. The charge state and recoil energy distribution measurements also involved appropriate variation of the HIRA fields. A charge resetting carbon foil was used to check for any possible effects caused by the presence of isomeric states. The energy distribution was also derived from the mass gated time-of-flight spectra obtained by γ-residue coincidences. For angular distribution of the residues, a solid angle of 1 msr was used in HIRA, and measurements were done on both sides of the incident beam direction to fix the true zero degree direction.

The cross sections for ER's were measured with a 5 msr solid angle in the HIRA in the energy range from 10% below the nominal Coulomb barrier to about 15% above the barrier. The HIRA fields were set to select the ER's with the optimum charge state. The fusion cross sections were obtained by summing up the contributions from the dominant channels, corresponding to evaporation of up to seven nucleons. These channels exhaust almost the entire fusion-evaporation cross section. A detailed comparison with the calculations employing the code CASCADE [19] justified this assumption except for the ^{58}Ni target at higher beam energies, where it is found that a significant fraction of the evaporation cross section consists of the nine-nucleon and ten-nucleon evaporation channels. These particular channels, which involve the emission of two α particles, have poor detection efficiencies because of rather broad energy and angular distribution of residues. A correction up to a maximum of 20% is applied in

TABLE III. Barrier parameters V_b and R_b for the systems ^{48}Ti+^{58,60,64}Ni. Errors for the experimental values are given in parentheses.

	Present Expt.		Akyüz-Winther		Vaz systematics	
System	V_b (MeV)	R_b (fm)	V_b (MeV)	R_b (fm)	V_b (MeV)	R_b (fm)
^{48}Ti+^{58}Ni	78.8 (0.3)	9.8 (0.3)	79.3	10.4	80.5	10.2
^{48}Ti+^{60}Ni	77.3 (0.3)	10.0 (0.3)	78.8	10.5	80.1	10.3
^{48}Ti+^{64}Ni	76.7 (0.3)	10.2 (0.3)	78.0	10.6	79.2	10.4

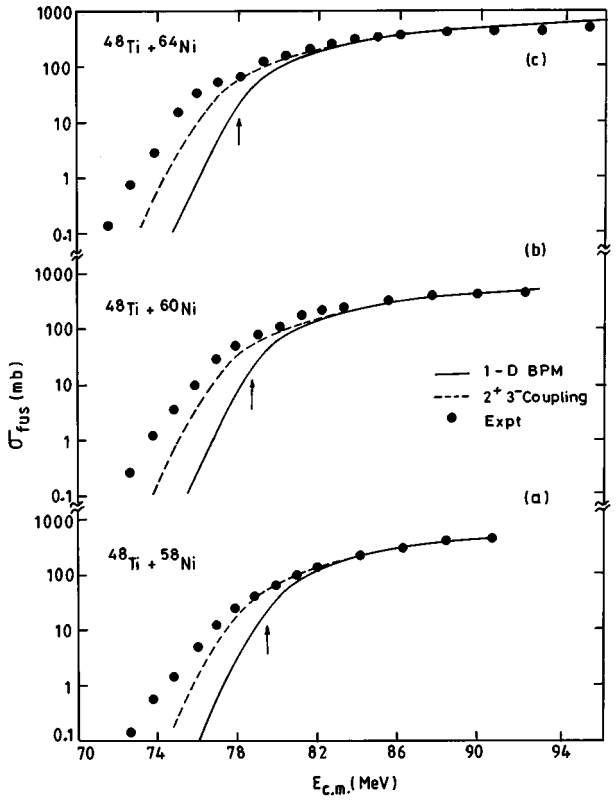

FIG. 4. Fusion excitation functions for the systems (a) ^{48}Ti $+^{58}$Ni, (b) ^{48}Ti$+^{60}$Ni, and (c) ^{48}Ti$+^{64}$Ni. The solid curves give the results of the 1D BPM calculations, and the dashed curves are the results of coupled channel calculations including couplings to the lowest 2^+ and 3^- states in the projectile and the target, using the CCMOD code. The fusion barriers are shown by the arrows. The statistical errors are within the size of the points.

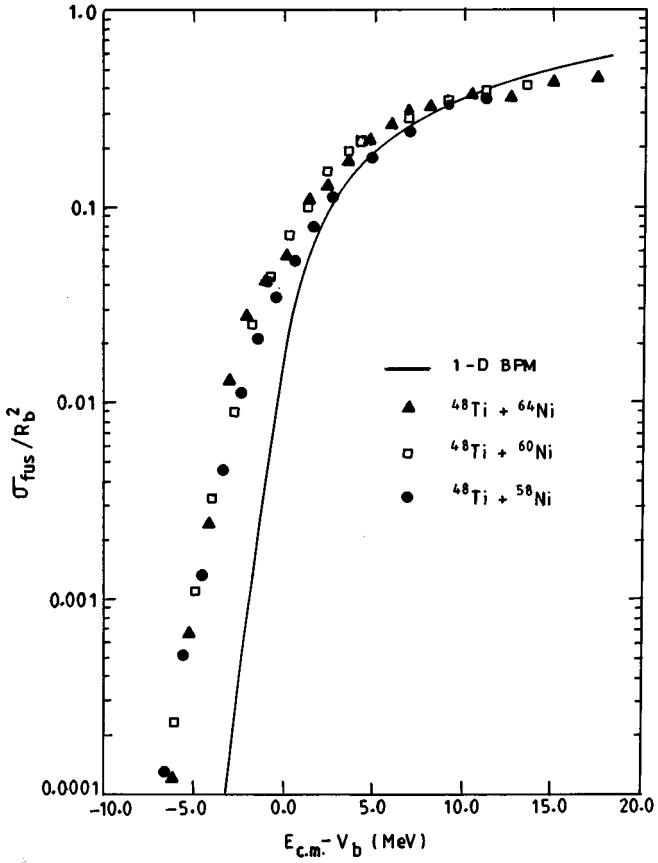

FIG. 5. Reduced plots of fusion excitation functions for the systems ^{48}Ti$+^{58}$Ni, ^{48}Ti$+^{60}$Ni, and ^{48}Ti$+^{64}$Ni. The parameters R_b and V_b are calculated using the Akyüz-Winther potential. The solid curve shows 1D BPM results.

order to account for these channels in the case of ^{58}Ni at high energies. The fission contribution is expected to be small and has been neglected.

The fusion cross section $\sigma_{\rm fus}$ was obtained by summing the contributions σ_i from different evaporation channels specified by the mass of the residues. The cross section σ_i for a given channel may be written as

$$\sigma_i = \frac{1}{\epsilon_i}\frac{Y_i}{C}\frac{d\sigma_R}{d\Omega}\Omega_M , \tag{1}$$

where Y_i is the yield of the ith evaporation channel, ϵ_i the average HIRA efficiency, C the monitor counts, Ω_M the solid angle subtended by the monitor, and $d\sigma_R/d\Omega$ the Rutherford differential cross section in the laboratory system.

A typical two-dimensional plot of the energy loss signal from MWPC vs the focal plane position is given in Fig. 1, showing a clear separation of the residues from the scattered beamlike particles. The M/q spectrum, with M and q being the mass and the charge state of the residues, is shown in Fig. 2. The mass assignment, done initially by using an α source [17], was confirmed by the coincident γ-ray spectra. Figures 3(a) and 3(b) give the γ-ray spectra gated by masses 102 and 103, respectively, showing the γ lines for the low-lying transitions in the corresponding residues. The singles γ-ray spectrum is given in Fig. 3(c). The ratio of the areas of the corresponding γ peaks in the gated and the singles spectra give the HIRA efficiency.

Absolute detection efficiency of the residues depends on several factors: (i) the distribution of various particle parameters such as their mass, energy, charge state, and angle and (ii) the energy, mass, and angular acceptances of the HIRA. Of these, only the former vary for different reactions, while the latter are purely instrument related. In the present mea-

TABLE IV. Excitation energies E_x and deformation parameters β of the states included in the coupled channel calculations.

Nucleus	State (J^π)	E_x (MeV)	β
^{48}Ti	2^+	0.98	0.269
	3^-	3.36	0.188
^{58}Ni	2^+	1.45	0.183
	3^-	4.48	0.175
^{60}Ni	2^+	1.33	0.207
	3^-	4.04	0.190
^{64}Ni	2^+	1.35	0.179
	3^-	3.56	0.230

surements, absolute detection efficiencies for various evaporation channels at different beam energies have been obtained by a combination of theoretical estimates of the energy and the angular distributions of residues, by experimental determination of these distributions for certain selected cases, and by direct determination using γ coincidences at the higher energies. Mutual consistency of these has been established for several cases. The HIRA detection efficiencies for three-nucleon (3N) and four-nucleon (4N) evaporation channels at a beam energy of 160 MeV are listed in Table I. The theoretical estimates based on calculations using the code PACE2 [20] agree reasonably well with the measured values of the efficiencies and have been used in the case of remaining evaporation channels and at the other beam energies.

III. RESULTS AND DISCUSSION

The measured values of the fusion cross sections for all the reactions studied are listed in Table II. The errors are about 15%, with predominant contributions caused by uncertainties in the HIRA efficiency determination. Correction for the beam energy loss in the target has been incorporated following an iterative procedure. The values of the barrier height V_b and radius R_b, extracted from the above barrier data by a least-squares fit using the expression based on classical sharp cutoff model, are listed in Table III. It is seen that the values of the parameters are lower than those obtained from the systematics [21] as well as the ones calculated with the potential of that of Akyüz and Winther [22]. Similar disagreement was reported earlier for other systems [14]. The observed disagreement could be attributed, in part, to the nuclear potential, which can be determined more precisely from elastic scattering data in the Coulomb barrier region. Also, the values of the parameters obtained by least-squares fit may be in error if the measurements do not extend to sufficiently high energies or if account is not taken of any systematic energy dependence of the detection efficiency or partial missing of the yields of some channels.

The fusion excitation functions, plotted in Fig. 4, show large enhancements in the sub-barrier region as compared to the predictions of the one-dimensional barrier penetration model with the barrier parameters calculated using the Akyüz and Winther parametrization of the ion-ion potential [22]. The dashed curves show the results of a simplified coupled channel calculation using the code CCMOD [23] including the first-order coupling to the inelastic excitations of the lowest 2^+ and 3^- states in the target and projectile. The values of the deformation parameters β_2 and β_3, taken from the literature [24,25], are listed in Table IV. The observed sub-barrier enhancements cannot be accounted for by these calculations.

A comparison of the fusion data for the reactions studied is made in Fig. 5, where purely geometrical effects are removed by plotting $\sigma_{\rm fus}/R_b^2$ vs $(E_{\rm c.m.}-V_b)$. It is clear that there is no significant isotopic dependence in the cross sections for the three Ni isotopes with the sub-barrier fusion enhancements being more or less similar. At energies around the barrier, some variations are apparent with the ^{60}Ni data lying in between those for ^{58}Ni and ^{64}Ni.

The residual asymptotic barrier shifts $\Delta B_{2^+3^-}$ have been

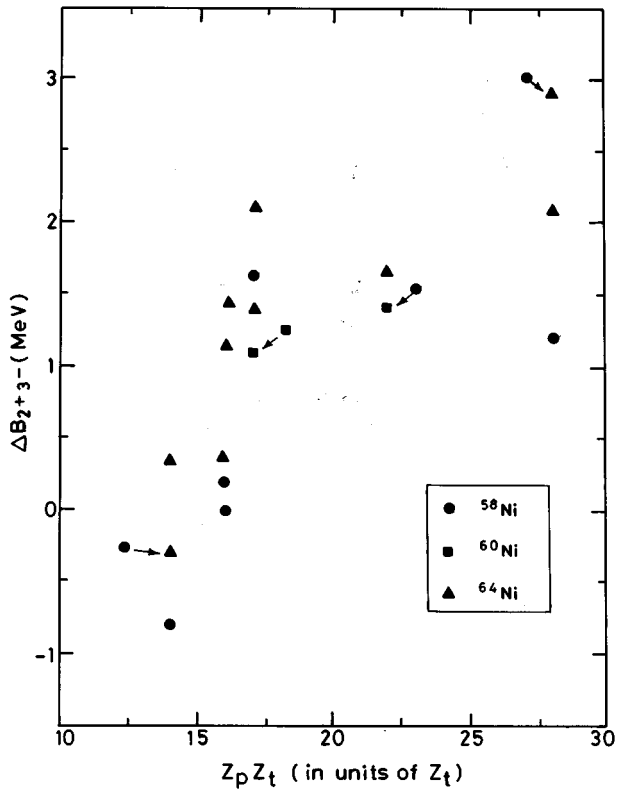

FIG. 6. Residual barrier shifts relative to CCMOD calculations including inelastic coupling to 2^+ and 3^- states in the projectiles and the targets for various systems involving nickel targets. The arrows indicate the merging of data points. The data for ^{28,30}Si and ^{32,36}S are from Ref. [14], for ^{35,37}Cl from Refs. [12,13,26], and for ^{58,64}Ni from Ref. [15]. The present data for ^{48}Ti projectile are also included.

calculated between the coupled channels and the experimental excitation functions at the 1 mb level. Figure 6 shows the residual shifts plotted against the product Z_pZ_t of the nuclear charges, which is taken as a measure of the nuclear overlap at the barrier. The data shown include measurements on Ni isotopes using the ^{28,30}Si, ^{32,36}S, ^{35,37}Cl, and ^{58,64}Ni beams [12–15,26] besides the ^{48}Ti beam from the present experiment. The $\Delta B_{2^+3^-}$ values gradually increase with the mass though sudden jumps are seen for a few beams on the ^{64}Ni target. In order to investigate the possible systematics underlying the residual asymptotic shifts, we have extracted for each beam, an ''average value'' taken over the Ni isotopes and a ''relative value'' defined as the difference for the ^{58}Ni and ^{64}Ni. The average $\Delta B_{2^+3^-}$, plotted in Fig. 7(a), shows an almost linear rise with a value close to zero for Si and $\sim$ 2.5 MeV for Ni beams. Experimental value from our measurements for the ^{48}Ti beam falls reasonably well on this line. On the other hand, the relative $\Delta B_{2^+3^-}$, plotted in Fig. 7(b), is seen to divide the reactions under consideration into two distinct sets. Set A, with large values around 1.4 MeV of the relative $\Delta B_{2^+3^-}$, consists of ^{28}Si, ^{32}S, ^{35}Cl, and ^{58}Ni beams. Set B, of the remaining beams, shows small values scattered around zero. All the beams belonging to set A have positive Q values for the two-neutron–pickup reaction to the ground state. The ^{48}Ti+^{64}Ni system also has a positive Q value for the $2n$-pickup reaction, and therefore should show

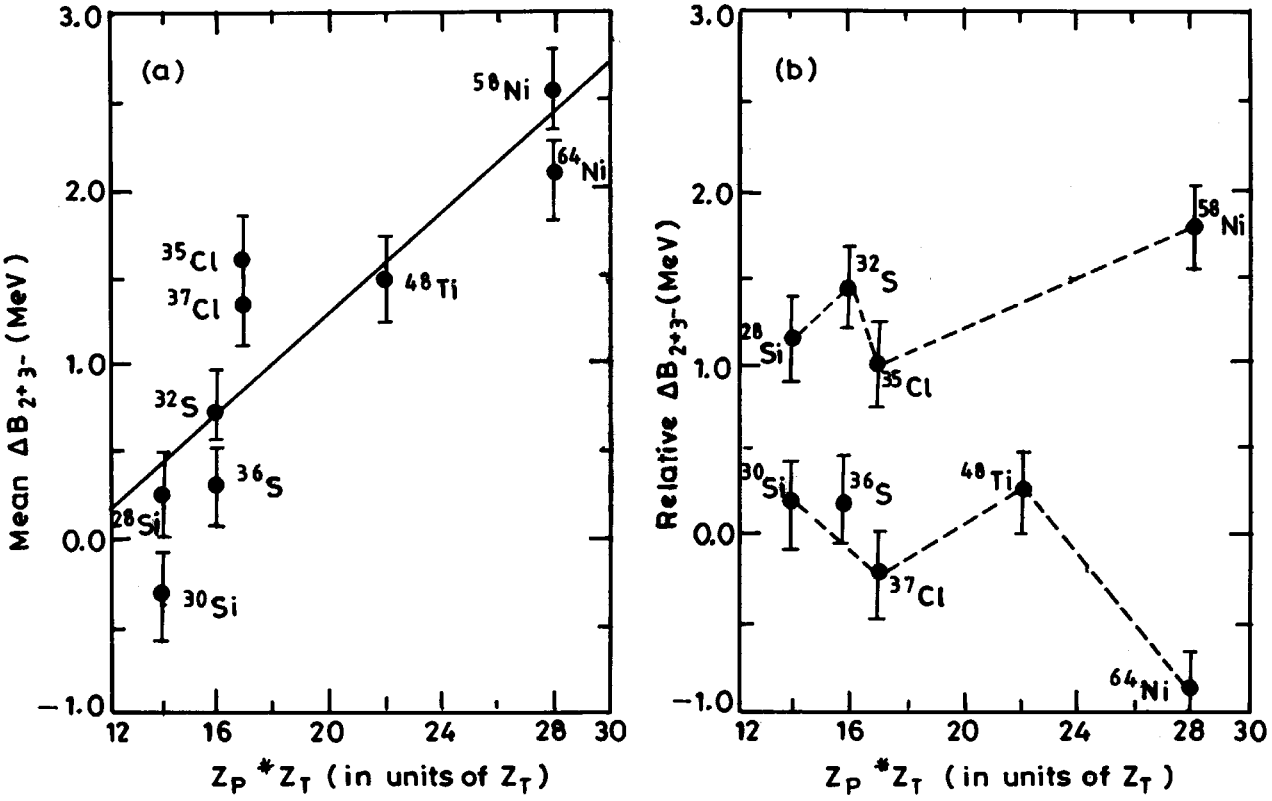

FIG. 7. (a) The average residual barrier shifts for ^{58}Ni and ^{64}Ni for given projectiles. (b) The difference in the residual barrier shifts for ^{58}Ni and ^{64}Ni for given projectiles.

up with additional enhancement having large ''relative $\Delta B_{2^+3^-}$''. However, the present measurements indicate that the ^{48}Ti beam does not show the additional enhancement for the ^{64}Ni target, quite in contrast to the case of the fusion of neighboring beams of set *A*.

A quantitative explanation of the observed lack of the additional enhancement for the ^{48}Ti+^{64}Ni system may be searched through coupled channel calculations involving transfer form factors obtained using the sub-barrier transfer data. However, in the absence of such a measurement, it would be worthwhile to speculate on any distinctive feature of the ^{48}Ti beam *vis-á-vis* beams of set *A*. One such aspect concerns a possible role of the ''*N/Z* equilibration,'' while the system is evolving towards fusion. It is interesting to note that for all the systems with positive *Q* values for the $2n$-pickup channel on ^{64}Ni, the *N/Z* values of the projectile-like and the target-like nuclei following the $2n$-pickup process remain intermediate between the *N/Z* values of the fused system and the corresponding initial nuclei, with the sole exception of the ^{48}Ti case. In the case of ^{48}Ti the $2n$-pickup process carries the *N/Z* values of the participants beyond that for the fused system, and thus may not contribute towards the fusion enhancement.

Besides the possible transfer-related additional enhancement for the beams of set *A* on ^{64}Ni target, the behavior of the average $\Delta B_{2^+3^-}$ [Fig. 7(a)] relates well with the extent of the nuclear overlap at the barrier. A modification in the ion-ion potential was attempted by adjusting the parameter dv [23] in order to understand this behavior. A value of dv, which reproduces the residual asymptotic barrier shift for ^{48}Ti, was found to overpredict the value for ^{28}Si by about 1 MeV. Thus it is not possible to account for the average $\Delta B_{2^+3^-}$ with a single set of values of the parameters specifying the heavy-ion potential, and the observed trend may be a manifestation of the increasing role of higher-order couplings [27].

A statistical model analysis of the experimental evaporation residue cross sections for the three systems has been carried out using the code CASCADE [19] following a method similar to that used by Dasgupta *et al.* [23]. The analysis requires the mean angular momentum $\langle \ell \rangle \hbar$ of the compound nucleus as a critical input for predicting the relative yields of the various evaporation channels. A triangular shape was assumed for the spin distribution, and the value of the mean angular momentum was adjusted so as to reproduce the ratio *R* of the observed yields of the four- and three-nucleon evaporation channels. The derived mean spin values are compared with the calculations in Fig. 8. Statistical model parameters were varied over a reasonable range to estimate the error in the derived $\langle \ell \rangle \hbar$ values. The estimated errors are found to be lowest for the ^{48}Ti + ^{64}Ni system and highest for the ^{48}Ti + ^{60}Ni system. For the lowest energies, where the ratio *R* becomes quite small, the inherent limitations of the method give larger uncertainties in the derived $\langle \ell \rangle \hbar$. It is seen from the figure that all the three systems show deviations from the predictions of 1D BPM. The simplified coupled channel calculations also do not reproduce the experimental mean spin values. This is evident in the case of ^{60}Ni and ^{64}Ni, although the errors do not permit a definite conclusion for the case of ^{58}Ni. The expected behavior of saturation at energies well below the barrier is clearly seen in the case of ^{58}Ni.

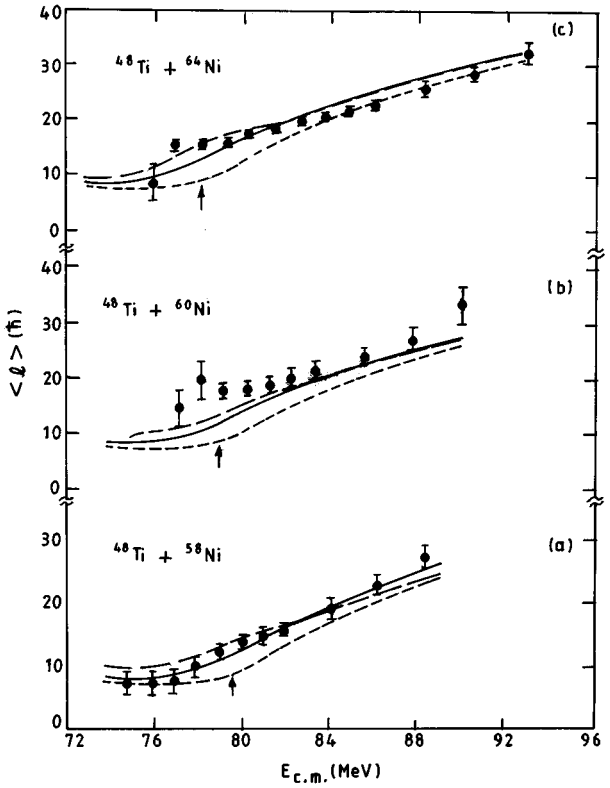

FIG. 8. Angular momentum distributions in the compound nucleus for the fusion of ^{48}Ti with ^{58,60,64}Ni targets. The filled circles are the experimental values derived from observed ratio of yields of evaporation residues for 4N and 3N channels. Long-dashed curves show the values derived from the fusion excitation function, whereas solid curves are the results of CCMOD calculations including the lowest inelastic excitations. The short-dashed curves represent 1D BPM results. The arrows indicate the fusion barriers.

Under certain reasonable assumptions, the spin distribution in the compound nucleus may be obtained from the shape of the excitation function [28]. We have extracted the mean spin values from the experimental excitation functions, following the procedure used by Ackermann *et al.* [29]. The results shown in Fig. 8 by the long-dashed curve, are found to be consistent with the values derived using the experimental ratio R.

IV. SUMMARY

The fusion process has been investigated at energies near and below the Coulomb barrier region for the systems ^{48}Ti+ ^{58,60,64}Ni. The absolute fusion cross sections have been derived from the yields of the various evaporation residues detected at the focal plane of the recoil mass separator, the HIRA. The fusion excitation functions for all the three systems show residual enhancements with respect to the results of simplified coupled channels calculations done by including the effects of first-order couplings to the lowest 2^+ and 3^- inelastic excitations of the colliding nuclei. The experimental ratios of the yields of the four- and three-nucleon evaporation channels were used to derive the mean angular momentum of the compound nucleus, with the help of statistical model calculations based on the code CASCADE. The derived mean spin values also show enhancements over coupled channel calculations, around the barrier region. However, the experimental data fail to show any marked isotopic dependence. A possible role of a few nucleon transfer couplings as well as higher-order–multiphonon couplings needs to be investigated.

ACKNOWLEDGMENTS

The authors thank the Pelletron accelerator crew at NSC for their support and excellent machine operation during the experiments. We acknowledge the help received from our colleagues Dr. A. Mandal, Mr. Ambuj Tripathi, and Mr. Mahendrajit Singh during the experiment. Comments and critical reading of the manuscript by Professor R. Singh (NEHU) are gratefully acknowledged. We thank Professor G. K. Mehta, Director, Nuclear Science Centre, for his constant interest and encouragement throughout this work. Two of us, A.M.V. and N.V.S.V.P. acknowledge with thanks the financial aid of the University Grants Commission and the Council of Scientific and Industrial Research, New Delhi, respectively.

[1] S. G. Steadman and M. J. Rhoades-Brown, Annu. Rev. Nucl. Part. Sci. **36**, 649 (1986).
[2] M. Beckerman, Rep. Prog. Nucl. Phys. **51**, 1047 (1988).
[3] W. Reisdorf, J. Phys. G **20**, 1297 (1994).
[4] R. Vandenbosch, Annu. Rev. Nucl. Part. Sci. **42**, 447 (1992).
[5] V. S. Ramamurthy, A. K. Mohanty, S. K. Kataria, and G. Rangarajan, Phys. Rev. C **41**, 2702 (1990); A. K. Mohanty, S. V. S. Shastry, S. K. Kataria, and V. S. Ramamurthy, Phys. Rev. Lett. **65**, 1096 (1990).
[6] H. Esbensen, Nucl. Phys. **A352**, 147 (1981).
[7] R. G. Stockstad, W. Reisdorf, K. D. Hildenbrand, J. V. Kratz, G. Wirth, R. Lucas, and J. Poitou, Z. Phys. A **295**, 269 (1980).
[8] C. E. Aguiar, V. C. Barbosa, L. F. Canto, and R. Donangelo, Nucl. Phys. **A472**, 571 (1987).
[9] C. H. Dasso, S. Landowne, and A. Winther, Nucl. Phys. **A405**, 381 (1983); **A407**, 221 (1983).
[10] C. H. Dasso and S. Landowne, Comput. Phys. Commun. **46**, 187 (1987); J. Fernandez-Niello and C. H. Dasso, *ibid.* **54**, 409 (1989).
[11] G. Galetti and M. A. Candido Ribeiro, Phys. Rev. C **50**, 2136 (1994), and other references therein.
[12] W. Scobel, H. H. Gutbrod, M. Blann, and A. Mignerey, Phys. Rev. C **14**, 1808 (1976).
[13] J. J. Vega, E. F. Aguilera, G. Murillo, J. J. Kolata, A. Morsad, and X. J. Kong, Phys. Rev. C **42**, 947 (1990).
[14] A. M. Stefanini, G. Fortuna, R. Pengo, W. Meczynski, G. Montagnoli, L. Corradi, A. Tivelli, S. Beghini, C. Signorini, S. Lunardi, M. Morando, and F. Soramel, Nucl. Phys. **A456**, 509 (1986).
[15] M. Beckerman, M. Salomaa, A. Sperduto, J. D. Molitoris, and

A. Di Rienzo, Phys. Rev. C **25**, 837 (1982); M. Kikora, M. Blann, W. Scobel, J. Bisplinghoff, and M. Beckerman, *ibid.* **25**, 885 (1982).
[16] S. Landowne, S. C. Pieper, and F. Videbaek, Phys. Rev. C **35**, 597 (1987).
[17] A. K. Sinha, N. Madhavan, J. J. Das, P. Sugathan, D. O. Kataria, A. P. Patro, and G. K. Mehta, Nucl. Instrum. Methods A **339**, 543 (1994).
[18] D. O. Kataria, A. K. Sinha, J. J. Das, N. Madhavan, P. Sugathan, G. Dayanand, M. C. Radhakrishna, A. M. Vinodkumar, K. M. Varier, Mahendrajit Singh, and N. V. S. V. Prasad, Nucl. Instrum. Methods A (to be published).
[19] F. Pühlhofer, Nucl. Phys. **A280**, 267 (1977).
[20] A. Gavron, Phys. Rev. C **21**, 230 (1980).
[21] L. C. Vaz, J. M. Alexander, and G. R. Satchler, Phys. Rep. **69**, 373 (1981).
[22] O. Akyüz and A. Winther, in *Proceedings of the Enrico Fermi International School of Physics, 1979*, edited by R. A. Broglia, C. H. Dasso, and R. Ricci (North-Holland, Amsterdam, 1981), p. 492.
[23] M. Dasgupta, A. Navin, Y. K. Agarwal, C. V. K. Baba, H. C. Jain, M. L. Jhingan, and A. Roy, Nucl. Phys. **A539**, 351 (1992); M. Dasgupta, Ph.D. thesis, Bombay University, Bombay, 1991.
[24] S. Raman, C. H. Malarkey, W. T. Milner, C. W. Nestor, and P. H. Stelson, At. Data Nucl. Data Tables **36**, 1 (1987).
[25] R. H. Spear, At. Data Nucl. Data Tables **42**, 55 (1989).
[26] R. J. Tighe, J. J. Vega, E. Aguilera, G. B. Liu, A. Morsad, and J. J. Kolata, Phys. Rev. C **42**, 1530 (1990).
[27] A. T. Kruppa, P. Romain, M. A. Nagarajan, and N. Rowley, Nucl. Phys. **A560**, 845 (1993).
[28] C. C. Sahm, H. G. Clerc, K. H. Schmidt, W. Reisdorf, P. Armbruster, F. P. Hessberger, J. G. Keller, G. Munzenberg, and D. Vermeulen, Nucl. Phys. **A441**, 316 (1985).
[29] D. Ackermann, F. Scarlssara, P. Bednerczyk, S. Beghini, L. Corradi, G. Montagnoli, L. Muller, D. R. Napoli, C. M. Petrache, K. M. Varier, F. Soramel, P. Spolaore, A. M. Stefanini, G. F. Segato, C. Signorini, and H. Zhang, Proceedings of the 5th International Conference on Nucleus-Nucleus Collisions, Italy, 1994 [Nucl. Phys. **A583**, 129 (1995)].